Fast Solid-State Li Ion Conducting Garnet-Type Structure Metal Oxides for Energy Storage

ARTICLE *in* JOURNAL OF PHYSICAL CHEMISTRY LETTERS · DECEMBER 2014

Impact Factor: 7.46 · DOI: 10.1021/jz501828v

4 AUTHORS:

Venkataraman Thangadurai
The University of Calgary
183 PUBLICATIONS **3,257** CITATIONS
SEE PROFILE

Dana Pinzaru
The University of Calgary
5 PUBLICATIONS **58** CITATIONS
SEE PROFILE

Sumaletha Narayanan
The University of Calgary
14 PUBLICATIONS **192** CITATIONS
SEE PROFILE

Ashok Kumar Baral
13 PUBLICATIONS **71** CITATIONS
SEE PROFILE

THE JOURNAL OF PHYSICAL CHEMISTRY Letters

Perspective

pubs.acs.org/JPCL

Fast Solid-State Li Ion Conducting Garnet-Type Structure Metal Oxides for Energy Storage

Venkataraman Thangadurai,* Dana Pinzaru, Sumaletha Narayanan, and Ashok Kumar Baral

Department of Chemistry, University of Calgary, 2500 University Drive Northwest, Calgary, Alberta, Canada T2N 1N4

ABSTRACT: Lithium ion batteries are the most promising energy storage system on the market today; however, safety issues associated with the use of flammable organic polymer-based electrolytes with poor electrochemical and chemical stabilities prevent this technology from reaching maturity. Solid lithium ion electrolytes (SLIEs) are being considered as potential replacements for the organic electrolytes to develop all-solid-state Li ion batteries. Out of the recently discovered SLIEs, the garnet-related structured Li-stuffed metal oxides are the most promising electrolytes due to their high total (bulk + grain boundary) Li ion conductivity, high electrochemical stability window (~6 V versus Li^+/Li at room temperature), and chemical stability against reaction with an elemental Li anode and high-voltage metal oxide Li cathodes. This Perspective discusses the structural−chemical composition−ionic conductivity relationship of Li-stuffed garnets, followed by a discussion on the Li ion conduction mechanism, as well as the electrochemical and chemical stability of these materials. The performance of a number of all-solid-state batteries employing garnet-type Li ion electrolytes is also discussed.

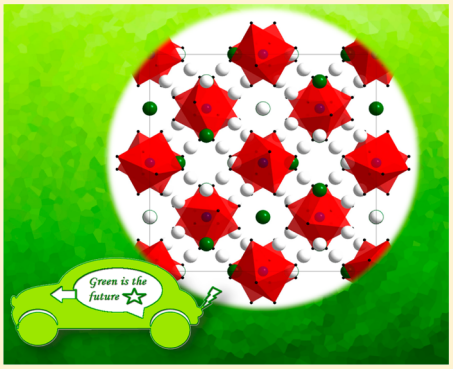

Electrolytes are ionic conductors and electronic insulators, named based on their conducting species such as F^-, OH^-, O^{2-}, H^+, Li^+, Na^+, K^+, Cu^+, Ag^+, and Mg^{2+}, and are broadly classified into solids and liquids. The solid electrolytes are further divided into amorphous and crystalline materials, while the liquid electrolytes can be generally classified into aqueous and nonaqueous (organic) electrolytes. The liquid electrolytes contain dissolved inorganic salts in water or organic solvents. The charge carriers are the solvated anions and cations. In the solid-state electrolytes, only one type of ionic species is the predominant charge carrier. For example, in well-known acceptor-doped fluorite-type ZrO_2 and perovskite-type $LaGaO_3$, the larger sized oxide ions are the main charge carriers, while the cations are part of the framework and do not contribute significantly to the total electrical conductivity.[1]

There is a need for the development of improved solid Li ion electrolytes (SLIEs) that possess all of the desired physical and chemical properties simultaneously.

Among the various known electrolytes, Li ion electrolytes (LIEs) are the most promising because elemental Li is the most electropositive and lightest of elements, thus, Li-based batteries offer the highest cell potential and gravimetric and volumetric energy densities.[2] Solid LIEs (SLIEs) are being considered as replacements for the commonly used organic polymer-based LIEs, with the advantages of miniaturization for portable electronic devices, chemical stability at higher temperatures, and lack of flammability, while being nonreactive under ambient atmosphere.[3−5] The practical physical and chemical properties sought after in the useful SLIEs include high total (bulk + grain boundary) Li ion conductivity of $\geq 10^{-3}$ S cm^{-1} with unit Li ion transference number ($t_{Li+} \approx 1$) over the entire range of Li activities (a_{Li}) from anode to cathode, negligible solid electrolyte−electrode interface (charge transport) impedance, electrochemical stability up to ~6 V versus Li^+/Li, and chemical stablity against reaction with Li battery electrodes. Shown in Figure 1 is the schematic representation of the desired functional properties of SLIEs for high-performance all-solid-state Li ion batteries. A large number of inorganic oxides and nonoxides exhibiting amorphous and crystalline structures have been investigated.[3−7] Table 1 lists the well-known examples of selected SLIEs as well as the merits and demerits in using them as electrolytes in all-solid-state Li ion batteries.[3,4,8] Thus, there is a need for the development of improved SLIEs that possess all of the desired physical and chemical properties simultaneously. The present paper gives perspective views of the most recently discovered garnet-type Li-stuffed metal-oxide-based SLIEs.

Li-Stuffed Garnet-Type Metal Oxides. Thangadurai et al. first observed Li ion conduction in the garnet-type Li-stuffed $Li_5La_3M_2O_{12}$ (M = Nb, Ta) in the $Li_2O−La_2O_3−M_2O_5$ system, which exhibits a bulk Li ion conductivity of $\sim 10^{-6}$ S cm^{-1} at 25 °C.[8] An ideal garnet structure has a general chemical formula of $A_3B_2C_3O_{12}$, where A (for, e.g., Ca, Mg, Y), B (for, e.g., Ga, Mn,

Received: August 29, 2014
Accepted: December 26, 2014

DOI: 10.1021/jz501828v
J. Phys. Chem. Lett. 2015, 6, 292−299

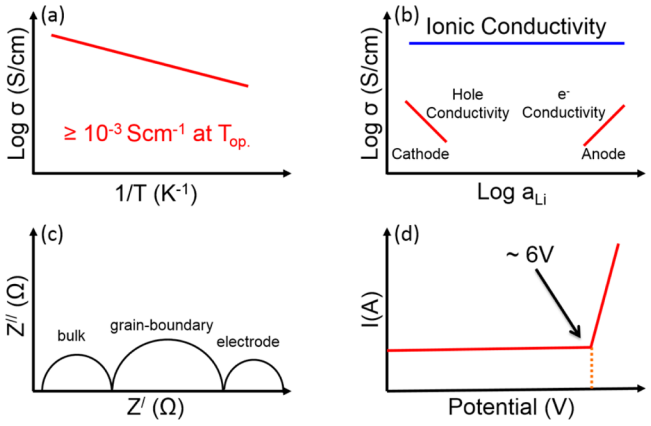

Figure 1. A schematic representation showing the desired electrical properties of solid Li ion electrolytes (SLIEs). SLIES should exhibit (a) high total ionic conductivity of $\geq 10^{-3}$ S cm^{-1} at the operating temperature (T_{op}) of the battery, (b) predominately Li ion conduction; electronic conductivity should be negligible over a wide range of Li ion activities, (c) negligible grain boundary contribution to total impedance and low electrolyte−electrode charge-transfer impedance, and (d) electrochemical stability up to 6 V.

Table 1. Well-Known SLIEs and Their Limiting Factors to Be Used in Solid State Li Ion Batteries[3,4,8]

SLIEs	limiting factors when employed in solid-state Li ion battery
Li_3N	very low decomposition voltage (0.44 V at RT) and isotropic conductivity
Li-β-alumina	hygroscopic, difficult to prepare as pure phase, and isotropic conductivity
$Li_{14}ZnGe_4O_{16}$	highly reactive with Li metal and atmospheric CO_2
$Li_{1.3}Ti_{1.7}Al_{0.3}P_3O_{12}$	unstable with Li metal, undergoes reduction of Ti^{4+} to Ti^{3+}, resulting in electronic short-circuit anode and cathode
$Li_{3x}La_{(2/3)-x}\square_{(1/3)-2x}TiO_3$	unstable with Li metal, undergoes reduction of Ti^{4+} to Ti^{3+}, resulting in electronic short circuit between the electrodes
$Li_{2.88}PO_{3.86}N_{0.14}$	moderate conductivity, prepared by using sputtering method, difficult to control the chemical composition for desired ionic conductivity

Ni, Fe, Al, Cr), and C (for, e.g., Al, Si, Ge, V) are eight-, six-, and four-oxygen-coordinated cation sites (Figure 2a). The availability of different coordination sites makes them suitable for different metal-ion-doping possibilities, as well as providing a platform for the understanding of the chemical composition−structure−functional property relationship. To the best of our knowledge, the first Li-based garnet-type metal oxides, $Ln_3M_2Li_3O_{12}$ (M = Te, W; Ln = lanthanides) were reported by Kasper in 1968,[9] while the Li excess garnets, $Li_5La_3M_2O_{12}$, were only discovered as Li ion conductors in 2003.[8] The idealized crystal structure of garnet-type $Li_5La_3M_2O_{12}$ is shown in Figure 2b.

In order to understand the effect of substitution on Li ion conductivity, a series of lanthanides (Ln = La, Pr, Nd, Sm, Eu) were used for complete substitution at the Ln sites in $Li_5Ln_3Sb_2O_{12}$.[10] Partial substitution of La with alkaline earth ions resulted in the composition $Li_6ALa_2M_2O_{12}$ (A = Ca, Sr, Ba, Mg, M = Nb, Ta).[11−13] The Ba-substituted Ta-based garnet showed a high electrochemical window of ~6 V versus Li^+/Li at 23 and 44 °C. The effect of lithium and oxygen concentration was studied for a family of compounds,

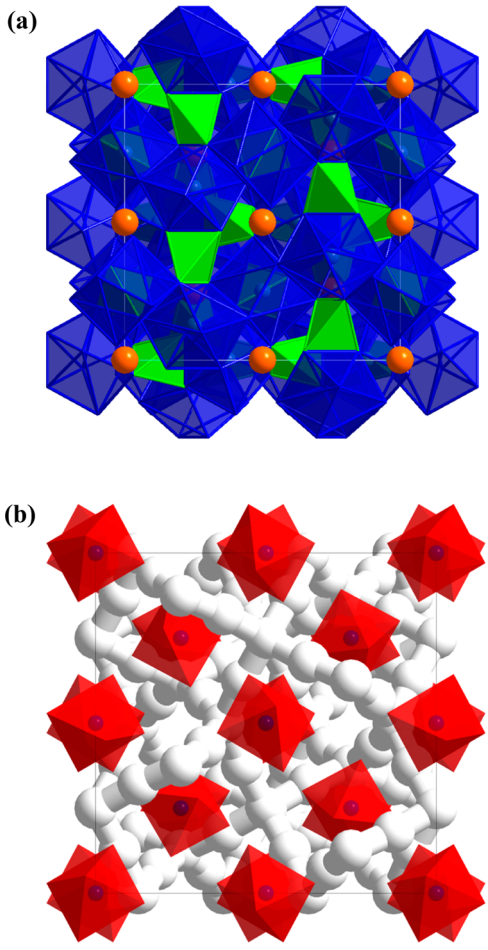

Figure 2. (a) Crystal structure of an ideal garnet of general formula $A_3B_2C_3O_{12}$, where the orange spheres represent B cations and blue and green polyhedrons represent A and C cations, respectively; (b) garnet-type $Li_5La_3M_2O_{12}$ where the white spheres represent Li cations, connected through channels representing possible Li migration pathways, and the red octahedra represent MO_6 units. La cations are omitted for clarity.

$Li_{5+x}Ba_xLa_{3-x}Ta_2O_{11.5+0.5x}$ (x = 0−2), and it was found that the conductivity is dependent on both lithium and oxygen concentration.[14] Another study showed that the ionic radius of the substituent affects both the crystal lattice constant and the Li ion conductivity of Li garnets.[15] The lattice parameter was also found to increase with increasing final sintering temperature for all substitutions in $Li_6ALa_2Ta_2O_{12}$ (A = Mg, Ca, Sr, $Sr_{0.5}Ba_{0.5}$, Ba), except the co-substitution by $Sr_{0.5}Ba_{0.5}$.[15]

Highly Li-stuffed $Li_7La_3Zr_2O_{12}$ crystallizes in cubic and tetragonal polymorphs. The sample synthesized at an elevated temperature of 1230 °C in air using an alumina crucible showed a cubic phase, while the one prepared at a lower temperature of 980 °C formed a tetragonal phase.[16,17] There are about 2 orders of magnitude difference in lithium ion conductivity between the two polymorphs at low temperatures. For example, the cubic $Li_7La_3Zr_2O_{12}$ showed a total conductivity of about 10^{-4} S cm^{-1} at room temperature, whereas the tetragonal $Li_7La_3Zr_2O_{12}$ showed a conductivity of ~10^{-6} S cm^{-1} at room temperature. When Zr was replaced with Sn in $Li_7La_3Zr_2O_{12}$, a similar temperature effect on the crystal structure was observed.[18] Recent studies show that the substitution with Al, Si, Ga, In, and Ge has an effect on the conductivity of cubic $Li_7La_3Zr_2O_{12}$.[19−22] A decrease in Li^+ conductivity was observed

DOI: 10.1021/jz501828v
J. Phys. Chem. Lett. 2015, 6, 292−299

with both Si and In doping; however, Al, Ge, and Ga doping doubled the Li^+ conductivity compared to the undoped $Li_7La_3Zr_2O_{12}$. The garnet-like $Li_{6.5}La_{2.5}Ba_{0.5}ZrTaO_{12}$ was synthesized by substitution of both La and Zr in the $Li_5La_3Ta_2O_{12}$, and the conductivity was found to have increased due to co-doping.[23]

A typical impedance plot of Li-stuffed garnets shows the bulk, grain boundary, and electrode contributions to the total conductivity at low temperature, as seen for $Li_{6.5}La_{2.5}Ba_{0.5}ZrTaO_{12}$ in Figure 3. The effect of oxide ion

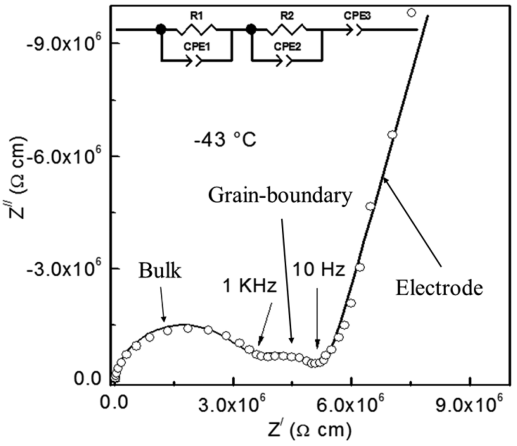

Figure 3. Typical impedance plot of garnet-type $Li_{6.5}La_{2.5}Ba_{0.5}ZrTaO_{12}$ at −43 °C. Bulk, grain boundary, and electrode responses can be well separated. This can be fitted using an equivalent circuit diagram composed of two sets of parallel resistor−capacitor components and a series capacitor. Reproduced by permission of The Royal Society of Chemistry from ref 23, copyright 2012.

vacancy on the ionic conductivity was studied on the composition $Li_5La_3Nb_{2-x}Y_xO_{12-\delta}$, by partially substituting Nb with Y in $Li_5La_3Nb_2O_{12}$.[24] Recent studies on Y substitution at the M sites of $Li_5La_3M_2O_{12}$ (M = Nb, Ta) produced Li-stuffed garnets with the general formula $Li_{5+2x}La_3M_{2-x}Y_xO_{12}$.[25,26] These studies supported the fact that ionic conductivity increases with Li content in the garnet structure. Figure 4

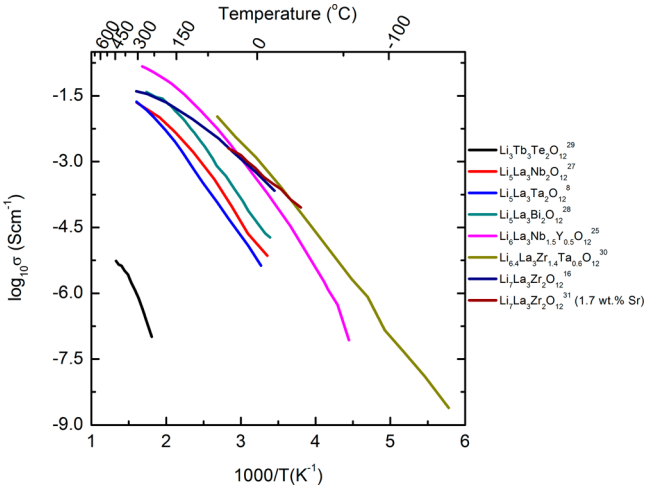

Figure 4. Extracted Li ion conductivity of garnet-type Li_3 ($Li_3Tb_3Te_2O_{12}$), Li_5 ($Li_5La_3M_2O_{12}$, where M = Nb, Ta, Bi), Li_6 ($Li_6La_3Nb_{1.5}Y_{0.5}O_{12}$), Li_{6+x} ($Li_{6.4}La_3Zr_{1.4}Ta_{0.6}O_{12}$), and Li_7 garnets ($Li_7La_3Zr_2O_{12}$ undoped and doped with 1.7 wt % Sr).[8,16,25,27−31]

shows the electrical conductivity of representative members of Li_3 ($Li_3Tb_3Te_2O_{12}$), Li_5 ($Li_5La_3M_2O_{12}$; M = Nb, Ta, Bi), Li_6 ($Li_6La_3Nb_{1.5}Y_{0.5}O_{12}$), Li_{6+x} ($Li_{6.4}La_3Zr_{1.4}Ta_{0.6}O_{12}$), and Li_7 ($Li_7La_3Zr_2O_{12}$ undoped and doped with 1.7 wt % Sr).[8,16,25,27−31] It is beyond the scope of this Perspective to report the conductivity of all of the known Li-stuffed garnets, which can be found in the recent critical review by Thangadurai et al.[32] Table 2 summarizes the Li ionic conductivity of some selected Li-stuffed garnet-type metal oxides with different Li concentrations.[32]

Both experimental and theoretical studies on Li-stuffed garnets have suggested that the Li ion conductivity as well as the migration pathways of the Li ions mainly depend on the Li content in the garnet-type materials and the Li distribution in the various crystallographic sites.

Lithium Ion Conduction Mechanism in Li-Stuffed Garnets. Both experimental and theoretical studies on Li-stuffed garnets have suggested that the Li ion conductivity as well as the migration pathways of the Li ions mainly depend on the Li content in the garnet-type materials and the Li distribution in the various crystallographic sites. There are three types of Li ion sites in the cubic garnet-type structure with a space group $Ia\bar{3}d$: (i) tetrahedral (24d), (ii) octahedral (48g), and (iii) off-centered octahedral (96h). Electrical conductivity studies show that the occupation of Li ions in the tetrahedral and octahedral sites directly control the ionic conductivity in the garnet-type materials (Figure 5).[32] However, Li-stuffed garnets with the same nominal compositions prepared at different laboratories show a couple of orders of magnitude variance in ionic conductivity that may be attributed to sample purity and/or differences in the density of the prepared materials.[32]

While studying the relation between Li ion occupancy and the Li ion conductivity in the lithium-stuffed garnets, O'Callaghan and Cussen[33] using the neutron diffraction studies found that the repulsive force between the Li ions in the tetrahedral sites and the octahedral sites leads to the displacement of Li^+ from the central 48g site to the off-centered 96h site within the octahedra. The number of Li ions displaced in the octahedral sites increases with increasing Li content in the materials, and the Li−Li repulsive interaction is responsible for the destabilization and the high mobility of Li^+ in the octahedral sites. In $Li_{3+x}Nd_3Te_{2-x}Sb_xO_{12}$, O'Callaghan et al. observed that the octahedral sites are connected to each other in a 3-D fashion such that Li conduction in the garnet structure is believed to occur exclusively via a network of edge-sharing distorted octahedra.[34]

Using ab initio calculations, Xu et al. have proposed two potential pathways (Route A and Route B) of Li ion migration in the cubic garnets.[35] In Route A, Li^+ migrates between two octahedral sites (Li(2)) via interstice bypassing their common tetrahedral neighbor (Li(1)), as shown in Figure 6.[26] This route seems to be favorable for $Li_5La_3Nb_2O_{12}$. Solid-state Li NMR studies further support that the conduction of Li ions occurs mostly between the octahedral sites, while the Li ions present

DOI: 10.1021/jz501828v
J. Phys. Chem. Lett. 2015, 6, 292−299

Table 2. Chemical Composition, Synthesis Temperature, Lattice Constant, and Li Ion Conductivity of Selected Garnets[a]

compound	lattice constant (Å)	σ (S cm^{-1})	E_a (eV)
$Li_3Tb_3Te_2O_{12}$ (900 °C)	12.35578(9)	4.4×10^{-6} (450 °C/air)	0.77(4)
$Li_5La_3Nb_2O_{12}$ (1100 °C)	12.718(2)	5.08×10^{-6} (22 °C/air)	0.60
$Li_5La_3Ta_2O_{12}$ (950 °C)	12.766(3)	1.2×10^{-6} (25 °C/air)	0.56
$Li_5Nd_3Sb_2O_{12}$ (925 °C)	12.66238(3)	1.3×10^{-7} (25 °C/air)	0.67
$Li_{5.5}La_3Nb_{1.75}In_{0.25}O_{12}$ (950 °C)	12.821(2)	1.8×10^{-4} (50 °C/air)	0.51
$Li_{5.5}La_{2.75}K_{0.25}Nb_2O_{12}$ (950 °C)	12.7937(8)	6.0×10^{-5} (50 °C/air)	0.49
$Li_6CaLa_2Nb_2O_{12}$ (900 °C)	12.697(2)	1.6×10^{-6} (22 °C/air)	0.55
$Li_6CaLa_2Ta_2O_{12}$ (1000 °C)	12.725(2)	2.2×10^{-6} (27 °C/air)	0.50
$Li_6BaLa_2Nb_2O_{12}$ (900 °C)	12.8893(2)	6.69×10^{-6} (22 °C/air)	0.42
$Li_6BaLa_2NbTaO_{12}$ (900 °C)	12.9897(5)	3.09×10^{-6} (25 °C/air)	0.47
$Li_6BaLa_2Ta_2O_{12}$ (900 °C)	12.946(3)	5.38×10^{-5} (22 °C/air)	0.40
$Li_6La_3SnSbO_{12}$ (1130 °C)	12.8991	2.2×10^{-5} (20 °C/air)	0.504
$Li_6La_3SnNbO_{12}$ (1130 °C)	12.8682	3.5×10^{-5} (20 °C/air)	0.503
$Li_6La_3SnTaO_{12}$ (1130 °C)	12.8693	4.2×10^{-5} (20 °C/air)	0.498
$Li_6SrLa_2Nb_2O_{12}$ (900 °C)	12.811(1)	4.2×10^{-6} (22 °C/air)	0.50
$Li_6SrLa_2Ta_2O_{12}$ (900 °C)	12.808(2)	8.84×10^{-6} (22 °C/air)	0.50
$Li_6CaLa_2Sb_2O_{12}$ (900 °C)	12.78594(12)	1.0×10^{-7} (95 °C/air)	0.82(3)
$Li_6La_3ZrTaO_{12}$ (1120 °C)	12.8873	2.5×10^{-4} (25 °C/air)	0.42
$Li_6La_3Zr_{1.5}W_{0.5}O_{12}$ (1100 °C)	12.94385	2.08×10^{-4} (30 °C/air)	0.46
$Li_{6.4}La_3Zr_{1.4}Ta_{0.6}O_{12}$ (1140 °C)	12.923	1.0×10^{-3} (25 °C/air)	0.35
$Li_{6.4}La_3Zr_{1.7}W_{0.3}O_{12}$ (1100 °C)	12.96507	7.89×10^{-4} (30 °C/air)	0.45
$Li_{6.5}La_{2.5}BaZrTaO_{12}$ (1100 °C)	12.783(4)	2.00×10^{-4} (23 °C/air)	0.31
$Li_{6.5}La_3Zr_{1.75}Te_{0.25}O_{12}$ (1100 °C)	12.9134	1.02×10^{-3} (30 °C/air)	0.38
$Li_{6.5}La_3Nb_{1.25}Y_{0.75}O_{12}$ (1100 °C)	12.9488(11)	2.7×10^{-4} (30 °C/air)	0.36
$Li_{6.55}La_3Hf_{1.55}Ta_{0.45}O_{13}$ (1130 °C)	12.9330(2)	3.45×10^{-4} (22 °C/air)	0.44
$Li_{6.6}La_3Zr_{1.6}Sb_{0.4}O_{12}$ (1100 °C)	12.95955	7.7×10^{-4} (30 °C/air)	0.34
$Li_{6.625}La_3Zr_{1.625}Ta_{0.375}O_{12}$ (1000 °C)	12.9438	5×10^{-4} (25 °C/air)	0.41
$Li_{6.7}La_3Zr_{1.7}Ta_{0.3}O_{12}$ (1130 °C)	12.9721	0.96×10^{-3} (25 °C/air)	0.37
$Li_{6.75}La_3Zr_{1.875}Te_{0.125}O_{12}$ (1100 °C)	12.9469	3.30×10^{-4} (30 °C/air)	0.41
$Li_{6.75}La_3Zr_{1.75}Nb_{0.25}O_{12}$ (1200 °C)	12.95	0.8×10^{-3} (25 °C/air)	0.31
$Li_7La_3Zr_2O_{12}$ (980 °C, tetragonal)	a = 13.134(4) c = 12.663(8)	1.63×10^{-6} (27 °C/air)	0.54
$Li_7La_3Zr_2O_{12}$ (1230 °C)	12.9682(6)	5.11×10^{-4} (25 °C/air)	0.32
$Li_7La_3Zr_2O_{12}$ (1.7 wt % Sr) (1200 °C)	12.980	5×10^{-4} (24 °C/air)	0.31
$Li_7La_3Sn_2O_{12}$ (900 °C, tetragonal)	a = 13.1206(1) c = 12.5467(1)	2.6×10^{-8} (85 °C/air)	0.79
$Li_7La_3Hf_2O_{13}$ (1000 °C, tetragonal)	a = 13.102(6) c = 12.630(2)	9.85×10^{-7} (23 °C/air)	0.53
$Li_7La_3Hf_2O_{13}$ (1250 °C)	12.938(1)	2.4×10^{-4} (23 °C/air)	0.29
$Li_7La_3Ta_2O_{13}$ (900 °C)	12.82	3.3×10^{-6} (27 °C/air)	0.38
$Li_7La_3Ta_2O_{13}$ (950 °C)	12.830(4)	5.0×10^{-6} (40 °C/air)	0.55
$Li_{7.06}La_3Zr_{1.94}Y_{0.06}O_{12}$ (1200 °C)	12.9672	9.56×10^{-4} (25 °C/air)	0.29
$Li_{7.06}La_3Zr_{1.94}Y_{0.06}O_{12}$ (950 °C)	12.974(3)	10^{-6} (23 °C/air)	0.47
$Li_{7.16}La_3Zr_{1.84}Y_{0.16}O_{12}$ (950 °C)	12.995(2)	10^{-6} (23 °C/air)	0.47

[a]Reproduced with permission from ref 32 (copyright 2014, Royal Society of Chemistry).

in the tetrahedral sites do not seem to be involved in the conduction mechanism.[32] In the second path, Route B, Li^+ moves through the shared triangular faces that separate the polyhedra around Li(1) and Li(2). The Li^+ migration in Route A is associated with an activation energy of ~0.6 eV and is preferred when Li^+ content is lower, such as Li_3 garnets. The activation energy of Li^+ in Route B is about 0.3 eV and is preferred in highly Li-stuffed $Li_7La_3Zr_2O_{12}$. Han et al. studied the Li ion migration pathways in cubic $Li_7La_3Zr_2O_{12}$ using high-temperature neutron diffraction and found that the conduction pathway contains both tetrahedral (24d) and octahedral sites. These results are consistent with the DFT studies by Xu et al.[35,36]

Recently, studies on the electrical transport properties of $Li_{5+2x}La_3Ta_{2-x}Y_xO_{12}$ (x = 0.25, 0.5, and 0.75) were found to be highly consistent with the theoretical prediction on the Li^+ migration pathway in the garnets with different Li content.[26] The activation energies for Li^+ migration obtained from the dipolar loss tangent analysis (0.69, 0.54, and 0.34 eV for $Li_{5.5}La_3Ta_{1.75}Y_{0.25}O_{12}$, $Li_6La_3Ta_{1.5}Y_{0.5}O_{12}$, and $Li_{6.5}La_3Ta_{1.25}Y_{0.75}O_{12}$, respectively) match well with the theoretical values for the different Li ion migration paths (Route A and Route B).[26,35] In a recent work, Wang et al. studied the mechanism of Li^+ diffusion in $Li_7La_3Zr_2O_{12}$ by using an internal friction method and suggested that one possible diffusion path could be directly between the 48g(96h) → 48g(96h) sites and the other between the 48g(96h) → 24d sites in the cubic garnets.[37]

Thangadurai et al. used the bond valence sum (BVS) model to identify the potential migration pathways of Li^+ ion in the garnet-type $Li_5La_3M_2O_{12}$ (M = Nb, Ta) and suggested that the 3-D Li^+ ion pathway network consists of nonplanar squares formed by the octahedral Li sites with an "almost" vacant tetrahedral site at the center, as shown in Figure 7.[38] It was assumed that all of the octahedral sites are fully occupied and the tetrahedral sites are almost vacant (partially occupied), which was found not to be the case, as confirmed by Cussen and Han et al. using neutron diffraction studies.[36,39] However, on the basis of ac impedance modulus spectroscopy analysis, the proposed motion of Li ions around the occupied tetrahedral

DOI: 10.1021/jz501828v
J. Phys. Chem. Lett. 2015, 6, 292−299

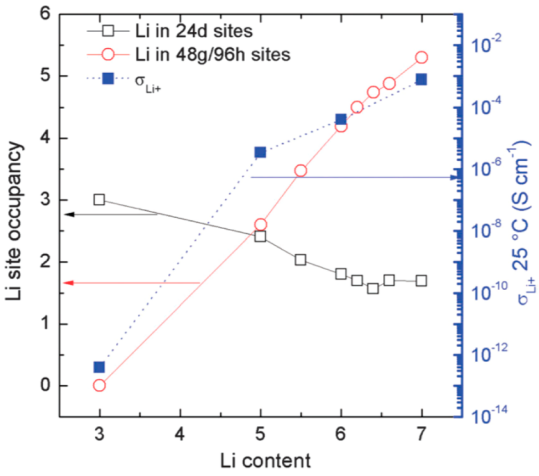

Figure 5. Variation of Li ion occupancy and room-temperature conductivity as a function of Li content in the garnet structure. The total conductivity values of representative garnets as a function of Li content are also shown ($Li_3Tb_3Te_2O_{12}$ (extrapolated), $Li_5La_3Ta_2O_{12}$, $Li_6BaLa_2Ta_2O_{12}$, and $Li_7La_3Zr_2O_{12}$). Reproduced by permission of The Royal Society of Chemistry from ref 32, copyright 2014.

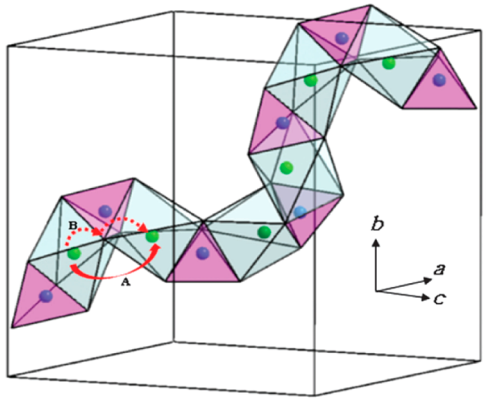

Figure 6. Connectivity of LiO_6 and LiO_4 polyhedra is shown. These polyhedra are connected in three dimensions throughout the unit cell. If there is a Li atom on a tetrahedral site, the Li atoms at the centers of neighboring octahedra (48g site) will be shifted to the 96h position to avoid close Li–Li contact. If the two octahedral sites that are on the two sides of a tetrahedral position are occupied, then the tetrahedral site between them will be empty. Arrows show two possible migration pathways A and B. Reproduced by permission of the PCCP Owner Societies from ref 26, copyright 2014.

sites support pathway involves both sites, and hence, they may be partially occupied.[26,38]

As a general characteristic of solid electrolytes, their conductivity obeys the Jonscher's universal power law (i.e., $\sigma = \sigma_{dc} + A\omega^n$, where σ_{dc} is the DC conductivity, ω is angular frequency, A is a constant, and n is the power factor that can have a value from 0 to 1).[40] According to the jump relaxation model, the hopping and the relaxation of ions give rise to conductivity dispersion at high frequencies.[41,42] In the case of Li garnets, the hopping of Li^+ seems to take place from the filled octahedral sites to the vacant octahedral sites, and after each jump, there exists Li^+ displacement from the central 48g positions to the 96h positions due to the repulsive interaction from the nearest Li^+ in the tetrahedral sites (24d). In this case, the Li^+ displacement can be considered to be part of the conductivity relaxation process of Li ions.

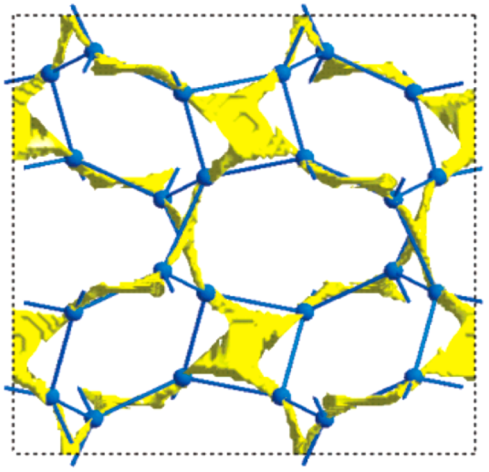

Figure 7. Bond valence models for Li^+ transport pathways in $Li_5La_3Nb_2O_{12}$ through the square formed by nonplanar fully occupied octahedra with unoccupied tetrahedra at the center. Reproduced with permission from ref 38, copyright 2004, American Chemical Society.

Using ac impedance dielectric spectroscopy, Baral et al. suggested that the Li ion displacement (from the 48g site to the 96h site) could cause a local charge polarization within the octahedral sites that leads to the existence of a net effective Li–Li electric dipolar interaction between the octahedral and tetrahedral sites.[26] The thermally activated motion of Li^+ from one octahedral site to another leads to the rotation of these electric dipoles. In the presence of an externally applied electric field, these arbitrarily oriented dipoles may be aligned, and may lead to the dipolar polarization loss. The migration energies for Li ions obtained from ac modulus spectra for $Li_{5.5}La_3Ta_{1.75}Y_{0.25}O_{12}$ and $Li_6La_3Ta_{1.5}Y_{0.5}O_{12}$ are similar to the activation energies associated with the dipolar rotations; therefore, the charge carriers involved in both the dipolar rotation and the local orientation process are considered to be the same. In the case of $Li_{6.5}La_3Ta_{1.5}Y_{0.5}O_{12}$, even though the modulus spectra mainly show the presence of long-range order migration of Li ions, the dielectric loss is still observed due to the continuous making and breaking of Li–Li dipoles during the long range order migration process.[26]

As far as the effect of lattice parameter on the conductivity of the garnets is concerned, it has often been observed that an increase in Li content increases the lattice parameter, leading to a facile path for Li^+ migration, as well as a reduction in the migration activation energy.[26] In a recent study, Zeier et al. observed that the unit cell parameter of $Li_6MLa_2Ta_2O_{12}$ (M = Ca, Sr, Ba) linearly increased with increasing ionic radius of the alkaline ions,[43] which is consistent with the findings of Thangadurai and Weppner in 2005.[11] A volume expansion in the dodecahedral $(La/M)O_8$, tetrahedral LiO_4, and octahedral LiO_6 sites was observed, with the exception of the TaO_6 polyhedra, which seems to result in the reduction of the activation energy for Li ion conductivity in $Li_6MLa_2Ta_2O_{12}$.[43]

Electrochemical and Chemical Stabilities of Li-Stuffed Garnets. DC polarization and cyclic voltammetry (CV) studies have shown that the Ta- and Zr-based Li-stuffed garnet-type oxides such as $Li_6La_2BaTa_2O_{12}$, $Li_7La_3Zr_2O_{12}$ (LLZ), and $Li_{7-x}La_3(Zr_{2-x}Nb_x)O_{12}$ exhibit an electrochemical stability window in the range of 5–9 V against Li electrodes.[11,16,44,45] Thangadurai et al. demonstrated an electrochemical stability window, up to 6 V versus Li/Li^+, for the Ba-doped garnet-type

DOI: 10.1021/jz501828v
J. Phys. Chem. Lett. 2015, 6, 292–299

$Li_6La_2BaTa_2O_{12}$ by Hebb–Wagner (HW) dc polarization measurements.[11] Shown in Figure 8a is the steady-state

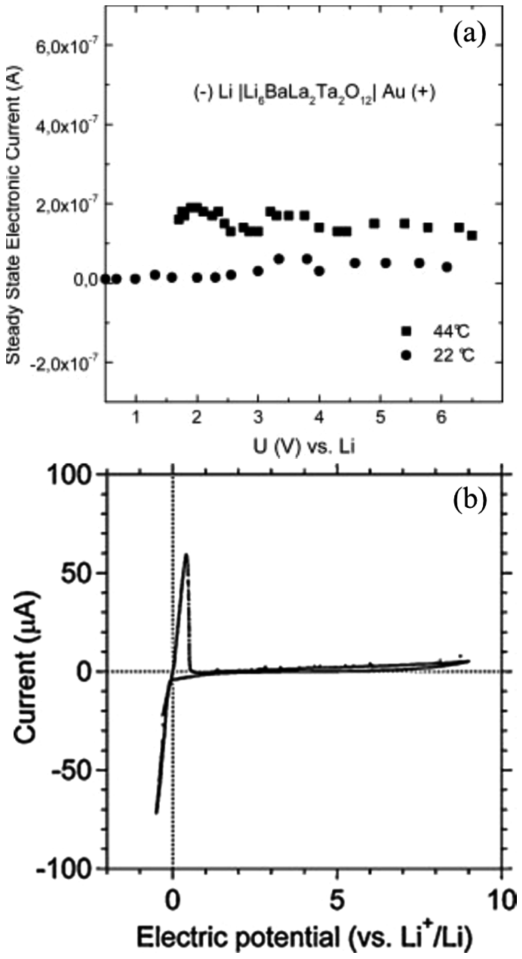

Figure 8. (a) Steady-state electronic current as a function of applied voltage for $Li_6BaLa_2Ta_2O_{12}$ obtained at 22 and 44 °C by HW measurements with a lithium ion-blocking electrode and using elemental lithium as the reference electrode. The measurements were performed inside of an argon-filled glovebox with an oxygen partial pressure of less than 1 ppm. Reprinted with permission from ref 11, copyright 2005. (b) A cyclic voltagram of $Li_{6.75}La_3(Zr_{1.75}Nb_{0.25})O_{12}$ bulk ceramic, recorded at a scanning rate of 1 mV s^{-1} at 25 °C. Reprinted with permission from ref 44, copyright 2011, Elsevier.

electronic current as a function of applied potential for the $Au/Li_6BaLa_2Ta_2O_{12}/Li$ cell. The lack of a sharp increase in the electronic current up to 6 V versus Li/Li^+ indicates that the garnet $Li_6La_2BaTa_2O_{12}$ material is electrochemically stable.[11] A similar result was reported for the cubic $Li_7La_3Zr_2O_{12}$ (LLZ) from the same group in 2007.[16] Several research groups using CV and dc methods further confirmed high electrochemical stability of Zr- and Ta-based Li-stuffed garnets.[44,45] Ohta et al. investigated the garnet-type Nb-doped $Li_{7-x}La_3(Zr_{2-x}Nb_x)O_{12}$ using CV.[44] No sharp peaks were observed up to 9 V versus Li/Li^+, suggesting a huge electrochemical stability window for $Li_{6.75}La_3Zr_{1.75}Nb_{0.25}O_{12}$ (Figure 8b).[44] Similar results have been reported for $Li_5La_3Ta_2O_{12}$, showing a stability window up to 5 V versus Li/Li^+.[45]

The chemical reactivity of garnet-like powdered $Li_6BaLa_2Ta_2O_{12}$ with powdered Li cathodes such as $LiCoO_2$, $LiMn_2O_4$, $LiNiO_2$, and $Li_2MMn_3O_8$ (M = Fe, Co) was studied using ex situ powder X-ray diffraction by Thangadurai and Weppner.[46] It was found that the Li garnet was chemically stable with the $LiCoO_2$ cathode up to 900 °C, while the other cathodes reacted with the electrolyte at temperatures above 400 °C. Similar results were reported by Narayanan et al. in 2012.[25] In this case, the garnet $Li_6La_3Nb_{1.5}Y_{0.5}O_{12}$ was used, and the cathode materials investigated were $Li_2CoMn_3O_8$ and $Li_2FeMn_3O_8$.

All-Solid-State Lithium Ion Batteries Based on Garnet-Like Li-Stuffed Electrolytes. Kotobuki et al. constructed an all-solid-state battery using $Li_7La_3Zr_2O_{12}$ (LLZ) solid electrolyte, a $LiCoO_2$ cathode, and elemental Li at the anode.[47] The interface resistance between the electrolyte and the anode was estimated from the chronopotentiograms to be about 5 kΩ at room temperature, which is 5 times higher than the resistance of the $Li_7La_3Zr_2O_{12}$ electrolyte alone obtained from impedance data. The $LiCoO_2/LLZ/Li$ cell showed reversible charge and discharge behaviors; however, this was reported over three cycles only. The maximum discharge capacity obtained with this cell was 0.2% of the full capacity estimated from the weight of the cathode.

In another study, Ohta et al. very successfully fabricated an all-solid-state battery using Li foil as the anode, a $LiCoO_2$ cathode, and a Nb-doped $Li_{6.75}La_3Zr_{1.75}Nb_{0.25}O_{12}$ garnet-type electrolyte.[48] The theoretical capacity of the cathode corresponding to 0.5 Li per $LiCoO_2$ is 137 mA h g^{-1}, and the capacity obtained experimentally with this battery was found to be 130 mA h g^{-1}, suggesting that 90% of the theoretical capacity was achieved. The solid-state Li battery was cycled 100 times, and the capacity after the 100th cycle was 127 mA h g^{-1}, which translates to about 98% retention capacity, confirming very good stable cycle performance of the battery, as shown in Figure 9.

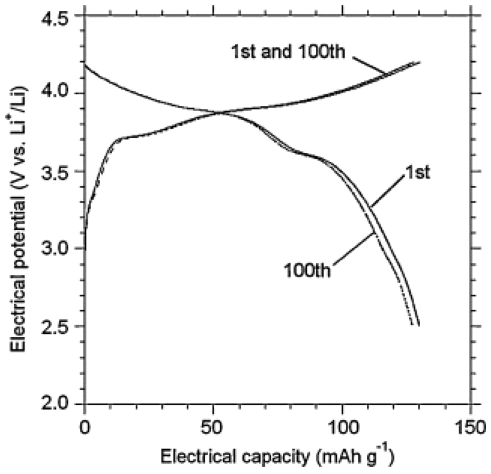

Figure 9. Charge–discharge curves for the $LiCoO_2/Li_{6.75}La_3Zr_{1.75}Nb_{0.25}O_{12}/Li$ cell. The horizontal axis shows the capacity normalized by the weight of the $LiCoO_2$ cathode. Solid and dotted lines represent the 1st and 100th charge–discharge cycles, respectively. Reprinted with permission from ref 48, copyright 2012, Elsevier.

Jin and McGinn prepared a solid-state battery by using a composite $Cu_{0.1}V_2O_5/Al$-LLZ/Li battery.[49] Compared to the previously used $LiCoO_2$, Cu-doped V_2O_5 has a much higher theoretical capacity (300 mA h g^{-1}). The battery tested at room temperature showed a discharge capacity of 53 mA h g^{-1}, which decreased to 4.9 mA h g^{-1} after five cycles, meaning that only

DOI: 10.1021/jz501828v
J. Phys. Chem. Lett. 2015, 6, 292–299

9.2% of the initial capacity was retained. When the working temperature was increased to 50 °C, the performance of the battery improved significantly, achieving an initial discharge capacity of 176 mA h g^{-1} that decayed much slower upon cycling.

Li-stuffed garnets remain as potential solid electrolyte candidates for high power and energy density all-solid-state Li ion batteries due to their high electrochemical stability window and their chemical stability against reaction with an elemental Li anode. Furthermore, these functional properties allow for the Zr- and Ta-based Li-stuffed garnets to be used as a Li protecting auxiliary electrolyte in Li–S and Li–air batteries.

In summary, Li-stuffed garnets remain as potential solid electrolyte candidates for high power and energy density all-solid-state Li ion batteries due to their high electrochemical stability window and their chemical stability against reaction with an elemental Li anode. Furthermore, these functional properties allow for the Zr- and Ta-based Li-stuffed garnets to be used as a Li protecting auxiliary electrolyte in Li–S and Li–air batteries. However, the challenge remaining is to prepare a dense garnet membrane without pinholes on Li metal anodes for practical applications. Further optimization of the chemical composition for higher ionic conductivity with excellent reproducibility and improvement to the processing methods are key to the commercialization of garnet materials. Li-stuffed garnets can potentially find applications in other solid-state ionic devices including gas sensors (e.g., CO_2)[50] and smart windows.

AUTHOR INFORMATION

Corresponding Author

*E-mail: vthangad@ucalgary.ca. Phone 1 403 210 8649.

Notes

The authors declare no competing financial interest.

Biographies

Dr. Venkataraman Thangadurai is an Associate Professor of Chemistry at the University of Calgary. He is a Fellow of the Royal Society of Chemistry, United Kingdom. He has received his Ph.D. from the Indian Institute of Science, Bangalore, India in 1999. He did his postdoctoral research at the University of Kiel and was supported by the Alexander von Humboldt (AvH) Foundation, Germany. He received his Habilitation degree from the University of Kiel in 2004. He was a visiting Associate Professor at the University of Maryland, College Park, U.S.A. in 2012–2013. His present research activities include developing novel solid electrolytes and mixed conductors for advanced energy conversion and storage devices, including solid oxide fuel cells, proton-conducting solid oxide fuel cells (H-SOFCs), all-solid-state Li ion batteries, as well as electrochemical gas sensors. http://www.ucalgary.ca/vthangad/

Dana Pinzaru was born and raised in the city of Bacau, Romania. She moved to Calgary, Canada in 2005. She is currently pursuing her M.Sc. degree at the University of Calgary under the supervision of Dr. V. Thangadurai. Her current research is focused on developing garnet-like solid Li ion electrolytes for all-solid-state Li ion batteries.

Sumaletha Narayanan received her M.Sc. degree from the University of Calgary, and she is currently pursuing her Ph.D. degree in Chemistry under the guidance of Dr. V. Thangadurai at the University of Calgary. Her research is focused on developing solid-state ionic conductors for all-solid-state Li ion batteries and proton-exchange membrane fuel cells.

Ashok Kumar Baral is a postdoctoral fellow in Dr. V. Thangadurai's group. He received his Ph.D. from the Indian Institute of Technology Madras (IITM), Chennai, India in 2010 and completed his postdoctoral research at Korea Institute of Science and Technology (KIST), Seoul, South Korea in 2012. His current research includes solid electrolytes and solid oxide fuel cell materials.

ACKNOWLEDGMENTS

The Natural Sciences and Engineering Research Council of Canada (NSERC) supported this work through the Discovery Grants (DG) program. One of us (V.T.) thanks Professor Dr. Werner Weppner at the Faculty of Engineering, University of Kiel, Germany for his constant support and encouragement to develop advanced solid-state electrolytes, including Li-stuffed garnet-type metal oxides and mixed conductors (electrodes) for energy storage, conversion, and gas sensor devices. V.T. also thanks Professors J. Gopalakrishnan and A. K. Shukla at the Solid State and Structural Chemistry Unit, Indian Institute of Science, Bangalore, India for their motivation. V.T. thanks Professors Stefan Adams (Department of Materials Science & Engineering, National University of Singapore), Martin Wilkening (Institute for Chemistry and Technology of Materials, Graz University of Technology), Peter Slater (School of Chemistry, University of Birmingham), Eric Wachsman (University of Maryland Energy Research Center, University of Maryland, College Park), and Reginald Paul (Department of Chemistry, University of Calgary) for their collaborations.

REFERENCES

(1) Jacobson, A. J. Materials for solid oxide fuel cells. *Chem. Mater.* **2009**, *22*, 660–674.

(2) Tarascon, J.-M.; Armand, M. Issues and challenges facing rechargeable lithium batteries. *Nature* **2001**, *414*, 359–367.

(3) Robertson, A.; West, A.; Ritchie, A. Review of crystalline lithium ion conductors suitable for high temperature battery applications. *Solid State Ionics* **1997**, *104*, 1–11.

(4) Thangadurai, V.; Weppner, W. Recent progress in solid oxide and lithium ion conducting electrolytes research. *Ionics* **2006**, *12*, 81–92.

(5) Takada, K. Progress and prospective of solid-state lithium batteries. *Acta Mater.* **2013**, *61*, 759–770.

(6) Goodenough, J. B.; Park, K.-S. The Li-ion rechargeable battery: A perspective. *J. Am. Chem. Soc.* **2013**, *135*, 1167–1176.

(7) Tatsumisago, M.; Nagao, M.; Hayashi, A. Recent development of sulfide solid electrolytes and interfacial modification for all-solid-state rechargeable lithium batteries. *J. Asian Ceram. Soc.* **2013**, *1*, 17–25.

(8) Thangadurai, V.; Kaack, H.; Weppner, W. Novel fast lithium ion conduction in garnet-type $Li_5La_3M_2O_{12}$ (M= Nb, Ta). *J. Am. Ceram. Soc.* **2003**, *86*, 437–440.

(9) Kasper, H. M. Series of rare earth garnets $Ln^{3+}{}_3M_2Li^{+}{}_3O_{12}$ (M = Te, W). *Inorg. Chem.* **1969**, *8*, 1000–1002.

(10) Percival, J.; Kendrick, E.; Slater, P. R. Synthesis and conductivities of the garnet-related li ion conductors, $Li_5Ln_3Sb_2O_{12}$ (Ln=La, Pr, Nd, Sm, Eu). *Solid State Ionics* **2008**, *179*, 1666–1669.

DOI: 10.1021/jz501828v
J. Phys. Chem. Lett. 2015, 6, 292–299

(11) Thangadurai, V.; Weppner, W. $Li_6ALa_2Ta_2O_{12}$ (A= Sr, Ba): Novel garnet-like oxides for fast lithium ion conduction. *Adv. Funct. Mater.* **2005**, *15*, 107−112.
(12) Murugan, R.; Thangadurai, V.; Weppner, W. Lithium ion conductivity of $Li_{5+x}Ba_xLa_{3-x}Ta_2O_{12}$ (x = 0−2) with garnet-related structure in dependence of the barium content. *Ionics* **2007**, *13*, 195−203.
(13) Percival, J.; Slater, P. R. Identification of the Li sites in the Li ion conductor, $Li_6SrLa_2Nb_2O_{12}$, through neutron powder diffraction studies. *Solid State Commun.* **2007**, *142*, 355−357.
(14) Murugan, R.; Thangadurai, V.; Weppner, W. Effect of lithium ion content on the lithium ion conductivity of the garnet-like structure $Li_{5+x}BaLa_2Ta_2O_{11.5+0.5x}$ (x = 0−2). *Appl. Phys. A: Mater. Sci. Process.* **2008**, *91*, 615−620.
(15) Murugan, R.; Thangadurai, V.; Weppner, W. Lattice parameter and sintering temperature dependence of bulk and grain-boundary conduction of garnet-like solid li-electrolytes. *J. Electrochem. Soc.* **2008**, *155*, A90−A101.
(16) Murugan, R.; Thangadurai, V.; Weppner, W. Fast lithium ion conduction in garnet-type $Li_7La_3Zr_2O_{12}$. *Angew. Chem., Int. Ed.* **2007**, *46*, 7778−7781.
(17) Awaka, J.; Kijima, N.; Hayakawa, H.; Akimoto, J. Synthesis and structure analysis of tetragonal $Li_7La_3Zr_2O_{12}$ with the garnet-related type structure. *J. Solid State Chem.* **2009**, *182*, 2046−2052.
(18) Percival, J.; Kendrick, E.; Smith, R. I.; Slater, P. R. Cation ordering in Li containing garnets: Synthesis and structural characterisation of the tetragonal system, $Li_7La_3Sn_2O_{12}$. *Dalton Trans.* **2009**, *26*, 5177−5181.
(19) El Shinawi, H.; Janek, J. Stabilization of cubic lithium-stuffed garnets of the type "$Li_7La_3Zr_2O_{12}$" by addition of gallium. *J. Power Sources* **2013**, *225*, 13−19.
(20) Huang, M.; Dumon, A.; Nan, C. W. Effect of Si, In and Ge doping on high ionic conductivity of $Li_7La_3Zr_2O_{12}$. *Electrochem. Commun.* **2012**, *21*, 62−64.
(21) Allen, J. L.; Wolfenstine, J.; Rangasamy, E.; Sakamoto, J. Effect of substitution (Ta, Al, Ga) on the conductivity of $Li_7La_3Zr_2O_{12}$. *J. Power Sources* **2012**, *206*, 315−319.
(22) Kumazaki, S.; Iriyama, Y.; Kim, K.-H.; Murugan, R.; Tanabe, K.; Yamamoto, K.; Hirayama, T.; Ogumi, Z. High lithium ion conductive $Li_7La_3Zr_2O_{12}$ by inclusion of both Al and Si. *Electrochem. Commun.* **2011**, *13*, 509−512.
(23) Narayanan, S.; Epp, V.; Wilkening, M.; Thangadurai, V. Macroscopic and microscopic Li^+ transport parameters in cubic garnet-type "$Li_{6.5}La_{2.5}Ba_{0.5}ZrTaO_{12}$" as probed by impedance spectroscopy and NMR. *RSC Adv.* **2012**, *2*, 2553−2561.
(24) Narayanan, S.; Thangadurai, V. Effect of Y substitution for Nb in $Li_5La_3Nb_2O_{12}$ on Li ion conductivity of garnet-type solid electrolytes. *J. Power Sources* **2011**, *196*, 8085−8090.
(25) Narayanan, S.; Ramezanipour, F.; Thangadurai, V. Enhancing Li ion conductivity of garnet-type $Li_5La_3Nb_2O_{12}$ by Y- and Li-codoping: Synthesis, structure, chemical stability, and transport properties. *J. Phys. Chem. C* **2012**, *116*, 20154−20162.
(26) Baral, A. K.; Narayanan, S.; Ramezanipour, F.; Thangadurai, V. Evaluation of fundamental transport properties of Li-excess garnet-type $Li_{5+2x}La_3Ta_{2-x}Y_xO_{12}$ (x = 0.25, 0.5 and 0.75) electrolytes using AC impedance and dielectric spectroscopy. *Phys. Chem. Chem. Phys.* **2014**, *16*, 11356−11365.
(27) Thangadurai, V.; Weppner, W. Effect of sintering on the ionic conductivity of garnet-related structure $Li_5La_3Nb_2O_{12}$ and In- and K-doped $Li_5La_3Nb_2O_{12}$. *J. Solid State Chem.* **2006**, *179*, 974−984.
(28) Murugan, R.; Weppner, W.; Schmid-Beurmann, P.; Thangadurai, V. Structure and lithium ion conductivity of bismuth containing lithium garnets $Li_5La_3Bi_2O_{12}$ and $Li_6SrLa_2Bi_2O_{12}$. *Mater. Sci. Eng., B* **2007**, *143*, 14−20.
(29) Cussen, E. J.; Yip, T. W. S.; O'Neill, G.; O'Callaghan, M. P. A comparison of the transport properties of lithium-stuffed garnets and the conventional phases $Li_3Ln_3Te_2O_{12}$. *J. Solid State Chem.* **2011**, *184*, 470−475.
(30) Li, Y.; Han, J.-T.; Wang, C.-A.; Xie, H.; Goodenough, J. B. Optimizing Li^+ conductivity in a garnet framework. *J. Mater. Chem.* **2012**, *22*, 15357−15361.
(31) Dumon, A.; Huang, M.; Shen, Y.; Nan, C.-W. High Li ion conductivity in strontium doped $Li_7La_3Zr_2O_{12}$ garnet. *Solid State Ionics* **2013**, *243*, 36−41.
(32) Thangadurai, V.; Narayanan, S.; Pinzaru, D. Garnet-type solid-state fast Li ion conductors for Li batteries: Critical review. *Chem. Soc. Rev.* **2014**, *43*, 4714−4727.
(33) O'Callaghan, M. P.; Cussen, E. J. Lithium dimer formation in the Li-conducting garnets $Li_{5+x}Ba_xLa_{3-x}Ta_2O_{12}$ ($0 < x \leq 1.6$). *Chem. Commun.* **2007**, *20*, 2048−2050.
(34) O'Callaghan, M. P.; Powell, A. S.; Titman, J. J.; Chen, G. Z.; Cussen, E. J. Switching on fast lithium ion conductivity in garnets: The structure and transport properties of $Li_{3+x}Nd_3Te_{2-x}Sb_xO_{12}$. *Chem. Mater.* **2008**, *20*, 2360−2369.
(35) Xu, M.; Park, M. S.; Lee, J. M.; Kim, T. Y.; Park, Y. S.; Ma, E. Mechanisms of Li^+ transport in garnet-type cubic $Li_{3+x}La_3M_2O_{12}$ (M = Te, Nb, Zr). *Phys. Rev. B* **2012**, *85*, 052301/1−052301/5.
(36) Han, J.; Zhu, J.; Li, Y.; Yu, X.; Wang, S.; Wu, G.; Xie, H.; Vogel, S. C.; Izumi, F.; Momma, K.; Kawamura, Y.; Huang, Y.; Goodenough, J. B.; Zhao, Y. Experimental visualization of lithium conduction pathways in garnet-type $Li_7La_3Zr_2O_{12}$. *Chem. Commun.* **2012**, *48*, 9840−9842.
(37) Wang, X. P.; Gao, Y. X.; Xia, Y. P.; Zhuang, Z.; Zhang, T.; Fang, Q. F. Correlation and the mechanism of lithium ion diffusion with the crystal structure of $Li_7La_3Zr_2O_{12}$ revealed by an internal friction technique. *Phys. Chem. Chem. Phys.* **2014**, *16*, 7006−7014.
(38) Thangadurai, V.; Adams, S.; Weppner, W. Crystal Structure Revision and Identification of Li^+-ion migration pathways in the garnet-like $Li_5La_3M_2O_{12}$ (M = Nb, Ta) oxides. *Chem. Mater.* **2004**, *16*, 2998−3006.
(39) Cussen, E. J. The structure of lithium garnets: Cation disorder and clustering in a new family of fast Li^+ conductors. *Chem. Commun.* **2006**, *4*, 412−413.
(40) Jonscher, A. K. The 'universal' dielectric response. *Nature* **1977**, *267*, 673−679.
(41) Dyre, J. C. The random free-energy barrier model for ac conduction in disordered solids. *J. Appl. Phys.* **1988**, *64*, 2456−2468.
(42) Funke, K. Ion transport in fast ion conductors — Spectra and models. *Solid State Ionics* **1997**, *94*, 27−33.
(43) Zeier, W. G.; Zhou, S.; Lopez-Bermudez, B.; Page, K.; Melot, B. C. Dependence of the Li-ion conductivity and activation energies on the crystal structure and ionic radii in $Li_6MLa_2Ta_2O_{12}$. *ACS Appl. Mater. Interfaces* **2014**, *6*, 10900−10907.
(44) Ohta, S.; Kobayashi, T.; Asaoka, T. High lithium ionic conductivity in the garnet-type oxide $Li_{7-X}La_3(Zr_{2-X}, Nb_X)O_{12}$ (X=0−2). *J. Power Sources* **2011**, *196*, 3342−3345.
(45) Kotobuki, M.; Kanamura, K. Fabrication of all-solid-state battery using $Li_5La_3Ta_2O_{12}$ ceramic electrolyte. *Ceram. Int.* **2013**, *39*, 6481−6487.
(46) Thangadurai, V.; Weppner, W. Investigations on electrical conductivity and chemical compatibility between fast lithium ion conducting garnet-like $Li_6BaLa_2Ta_2O_{12}$ and lithium battery cathodes. *J. Power Sources* **2005**, *142*, 339−344.
(47) Kotobuki, M.; Munakata, H.; Kanamura, K.; Sato, Y.; Yoshida, T. Compatibility of $Li_7La_3Zr_2O_{12}$ solid electrolyte to all-solid-state battery using li metal anode. *J. Electrochem. Soc.* **2010**, *157*, A1076−A1079.
(48) Ohta, S.; Kobayashi, T.; Seki, J.; Asaoka, T. Electrochemical performance of an all-solid-state lithium ion battery with garnet-type oxide electrolyte. *J. Power Sources* **2012**, *202*, 332−335.
(49) Jin, Y.; McGinn, P. J. $Li_7La_3Zr_2O_{12}$ electrolyte stability in air and fabrication of a $Li/Li_7La_3Zr_2O_{12}/Cu_{0.1}V_2O_5$ solid-state battery. *J. Power Sources* **2013**, *239*, 326−331.
(50) Zhu, Y.; Thangadurai, V.; Weppner, W. Garnet-like solid state electrolyte $Li_6BaLa_2Ta_2O_{12}$ based potentiometric CO_2 gas sensor. *Sens. Actuators, B* **2013**, *176*, 284−289.

DOI: 10.1021/jz501828v
J. Phys. Chem. Lett. 2015, 6, 292−299